

SiftMoE: Similarity-Aware Energy-Efficient Expert Selection for Wireless Distributed MoE Inference

Qian Chen, *Member, IEEE*, Xianhao Chen, *Member, IEEE*, and Kaibin Huang, *Fellow, IEEE*

Abstract—Mixture-of-Experts (MoE) architectures leverage sparse activation to enhance the scalability of large language models (LLMs), making them suitable for deployment in resource-constrained edge networks. However, the sheer number of experts often exceeds the memory capacity of individual edge nodes, necessitating wireless distributed MoE (WIDE) inference where experts are spread across multiple edge nodes. In this context, expert selection directly affects communication costs. Motivated by the similarity of experts, we propose SiftMoE, which judiciously selects or skips experts to strike a tradeoff between communication costs and inference accuracy. Specifically, we first establish theoretical bounds on the accuracy degradation resulting from expert replacement or skipping. Based on the bounds, we formulate an energy minimization problem for expert selection in WIDE inference subject to latency and accuracy constraints. In particular, for slow-fading channels, we derive optimal expert selection policies for both single-token decoding and multi-token prefilling. For fast-fading channels, we further extend our scheme to cope with rapidly varying channel conditions. Simulation results demonstrate that SiftMoE significantly reduces energy consumption while maintaining inference accuracy compared with conventional Top-K routing in WIDE systems.

Index Terms—Large language models, mixture-of-experts, expert selection, edge inference.

I. INTRODUCTION

Large language models (LLMs) have demonstrated remarkable performance across a range of intelligent applications, including natural language processing, autonomous driving, healthcare, and embodied AI [1], [2]. Motivated by stringent latency requirements and growing privacy concerns, pushing LLMs from cloud to the network edge is becoming a trend [3]–[5]. However, deploying such large models at the edge remains fundamentally challenging due to severe constraints on computation, memory, and energy resources of edge devices [6]–[8]. To alleviate these limitations, Mixture-of-Experts (MoE) architectures have recently emerged as a promising paradigm [9]. In MoE models, each transformer layer replaces the conventional single feed-forward network (FFN) with multiple expert networks, activating only a small subset for each input token. Due to their sparse activation patterns, MoE models enable substantial performance improvements while maintaining a computational budget comparable to that of conventional dense LLMs [10]. This property makes MoE models particularly appealing for scalable and efficient LLM deployment in resource-constrained edge environments [11].

Despite their advantages, a primary difficulty in MoE arises from the massive memory footprint incurred by the large number of experts, which often exceeds the memory capacity of a single edge node [12]–[14]. This limitation has motivated wireless distributed MoE (WIDE) frameworks, where experts are placed across multiple edge nodes to enable collaborative MoE inference [15], [16]. However, once experts are distributed across the edge network, expert activation decisions become tightly coupled with wireless communications, as the selected experts determine the links traversed and hence the associated transmission costs [17]. Conventional Top- K routing policies, which select K highest-scoring experts per layer based solely on model-internal gating scores [18], neglect channel states and may route hidden states to experts over poor-quality links, leading to excessive communication energy consumption and latency.

These limitations of fixed Top- K routing in wireless edge networks naturally raise a fundamental question: *can expert selection be redesigned to explicitly account for communication constraints and channel dynamics?* Recent empirical studies on MoE inference reveal that not all experts within the Top- K set contribute equally to output quality [19], [20]. The highest-ranked expert often dominates the prediction, while the lower-ranked experts yield only marginal performance gains. Meanwhile, many works on expert merging have shown that experts within the same layer exhibit substantial functional overlap [21], [22]. Such redundancy mainly arises from mechanisms used during training. Specifically, since load-balancing regularization disperses semantically similar tokens across multiple experts, the resulting homogeneous inputs lead to similar gradient updates, thus driving their parameters in similar directions. Top- K routing further amplifies this effect by repeatedly activating several experts for the same token. Taken together, these observations indicate that expert activation need not strictly follow conventional Top- K routing and can instead be made more flexible without significantly sacrificing inference accuracy. This flexibility, in turn, opens new opportunities for communication-aware expert selection in WIDE inference.

Existing studies on expert selection during MoE inference beyond conventional Top- K routing mainly investigate the *tradeoff between computation cost and inference accuracy* [11], [23]–[25]. A first class of approaches reduces the number of activated experts by skipping those deemed less critical within the original Top- K set, thereby decreasing computation and memory-access overhead. Specifically, candidate experts are sorted in descending order of their gating scores, and only the fewest top-ranked experts required to

Q. Chen, X. Chen, and K. Huang are with the Department of Electrical and Computer Engineering, The University of Hong Kong, Hong Kong (Email: qchen@eee.hku.hk, xchen@hku.hk, and huangkb@hku.hk). Corresponding authors: X. Chen and K. Huang.

reach a cumulative probability threshold are activated, while the remaining experts are suppressed to avoid unnecessary computation [23]. AdapMoE further characterizes expert importance via second-order sensitivity of the loss with respect to expert outputs, retaining highly sensitive experts while gating off low-sensitivity ones to reduce inference cost with minimal accuracy degradation [24]. In practical MoE implementations, a substantial portion of latency arises from repeatedly loading expert parameters from CPU memory into the GPU [26]. Motivated by this observation, another class of approaches replaces low-importance active experts with alternatives already resident in GPU memory that provide similar functionality, thereby avoiding frequent expert loading and eviction while maintaining output quality. Specifically, an importance-driven dual-priority scheduling algorithm quantifies each expert’s contribution using real-time routing scores [25]. Complementarily, the parameter committee framework exploits the temporal locality and functional exchangeability of experts to maintain a prioritized resident subset, where non-resident experts are either substituted by functionally similar counterparts or strategically skipped to eliminate I/O overhead during continuous inference [11]. Only a limited number of recent works further incorporate *wireless communication resources* into expert selection during inference [27], [28]. WDMoE compares the router weight vector with the latency vector using cosine similarity after Top- K routing, and removes the lowest-weight expert when the similarity falls below a predefined threshold, thereby reducing communication costs [27]. By jointly accounting for task relevance and wireless channel states, another work addresses expert selection across distributed nodes to minimize transmission energy under layer-wise quality-of-service (QoS) constraints [28].

In practice, selection-induced errors may accumulate and propagate across MoE layers, with different layers exhibiting heterogeneous sensitivity to the errors [19], [29], [30]. Consequently, it is essential to perform rigorous theoretical analysis to inform expert selection, thereby preserving inference accuracy. However, prior works on resource- and communication-aware expert selection for MoE inference primarily rely on heuristic similarity or importance metrics (e.g., cosine similarity, Hessian-based sensitivity, or routing scores), while lacking theoretical performance guarantees. To bridge this gap, this paper first develops a theoretical framework to quantify the effect of expert replacement or skipping on accuracy in WIDE inference. Building on this analysis, we then propose a similarity-aware energy-efficient expert selection framework for wireless distributed MoE (SiftMoE) inference. By exploiting functional similarity among experts within each MoE layer, SiftMoE integrates rigorous error analysis with channel-aware optimization to determine when experts should be replaced or skipped, thereby enabling energy-efficient inference under wireless fading while preserving accuracy. The main contributions of this work are summarized as follows.

- **Theoretical error analysis of expert selection:** We establish the *first* theoretical analysis of how expert selection affects output deviations in WIDE inference. Our analysis reveals two fundamental insights. First, experts

with small routing weights contribute marginally to the output, implying that removing or replacing them causes only limited distortion. Second, expert replacement is beneficial only when a functionally similar alternative exists; otherwise, directly skipping the expert may yield a tighter error bound. These results provide theoretical guidance for expert selection across layers under resource constraints.

- **Optimal expert selection under slow fading:** Based on the analysis above, we formulate an energy minimization problem over expert selection that accounts for wireless fading, latency constraints, and accuracy guarantees induced by similarity-aware replacement or skipping. For the slow-fading scenario, where channel conditions remain unchanged upon propagating each MoE layer, we design efficient algorithms to obtain optimal expert selection schemes for single-token decoding and multi-token prefilling phases, respectively.
- **Expert selection and adaptive transmission under fast fading:** For the fast-fading scenario, where channel states vary within each MoE layer, we reformulate the problem as minimizing the expected energy consumption subject to latency and accuracy constraints. Since jointly optimizing expert selection and transmission is difficult due to stochastic channel variations, we introduce a deterministic surrogate of the expected transmission energy to determine expert selection, whose structure is identical to the slow-fading problem. Then, we employ a dynamic programming (DP) approach to determine the optimal number of transmitted bits in each time slot.
- **Experimental results:** We conduct extensive experiments using state-of-the-art MoE models and real-world datasets to evaluate the proposed framework under wireless edge deployment scenarios. Compared with conventional Top- K routing, SiftMoE achieves higher inference accuracy while significantly reducing communication energy consumption under both slow- and fast-fading scenarios.

The remainder of this paper is organized as follows. Section II presents the WIDE inference architecture together with the communication, computation, and energy models. Section III establishes theoretical error bounds for expert selection. Building on these results, Section IV studies the energy-efficient expert selection scheme under slow fading. Then, Section V extends the framework to fast-fading environments and develops a joint expert selection and adaptive transmission scheme. Section VI presents experimental results and Section VII concludes the paper.

II. SYSTEM MODEL

As shown in Fig. 1, we consider a WIDE inference system including one user and a set of $N - 1$ helpers, denoted by $\mathcal{N} = \{1, \dots, N - 1\}$. Let $\mathcal{V} \triangleq \{\text{UE}\} \cup \mathcal{N}$ denote the set of all edge nodes, consisting of the user and all helpers, with $|\mathcal{V}| = N$. The user generates an inference task composed of M input tokens, indexed by the set $\mathcal{M} = \{1, \dots, M\}$. The inference task should be processed by an MoE model to generate the output results. The MoE model has L MoE

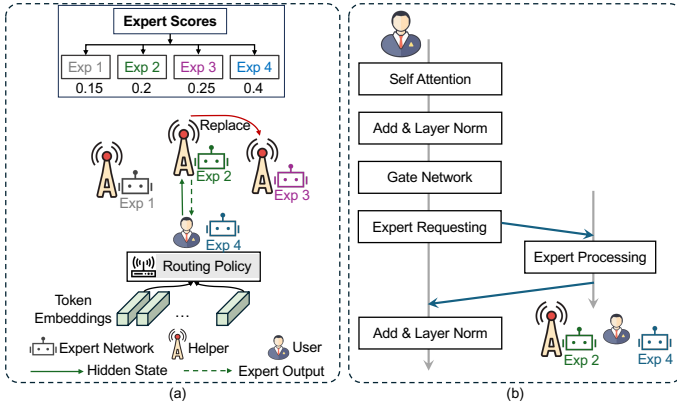


Fig. 1. An illustration of the WIDE inference system, where a user sends its tokens to the helpers with the required experts for processing. (a) The proposed SiftMoE framework, where “Exp” denotes expert. Here, expert 2 has a similar function but better channel condition compared with expert 3. (b) Operations of inference within an MoE layer.

layers, indexed by $\mathcal{L} = \{1, \dots, L\}$. Each MoE layer $\ell \in \mathcal{L}$ contains N experts, and the expert set of layer ℓ is denoted by $\mathcal{E}^{(\ell)} = \{1^{(\ell)}, \dots, N^{(\ell)}\}$. The experts are distributed across the edge nodes. Due to GPU memory constraints and parallel processing requirements, we assume that each edge node can load and execute at most one expert from each MoE layer at any given time [17], [27], [31]. Moreover, different edge nodes host distinct experts within the same layer, establishing a one-to-one mapping between experts and nodes. Consequently, selecting an expert in layer ℓ uniquely determines the edge node responsible for executing it, which simplifies our formulation.

As shown in Fig. 2, at each MoE layer, the attention and gating networks are first executed at the user to determine which experts are activated. Hosting attention and gating networks on edge devices enhances user privacy by remaining raw data locally. Since attention and gating operations incur a fixed computational workload per layer, their processing latency and energy consumption are treated as constants and excluded from the subsequent analysis. If a selected expert resides on a helper rather than the user, the hidden states are exchanged between the user and the helper. We use b to denote the data size of the transmitted hidden state per token.

A. Local Computing Model

We first consider the case where a token activates local experts at the user. In this case, the inference consists of two stages: i) loading the expert into the user’s GPU memory with latency $T_{\text{UE,load}}$, and ii) performing local expert computing.

Let $x_{m,\text{UE}}^{(\ell)}$ be a binary variable indicating whether token m is processed by the local expert of MoE layer ℓ . Specifically, $x_{m,\text{UE}}^{(\ell)} = 1$ if token m activates the local expert at layer ℓ , and $x_{m,\text{UE}}^{(\ell)} = 0$ otherwise. Then, the number of tokens processed locally at layer ℓ is given by $D_{\text{UE}}^{(\ell)} = \sum_{m \in \mathcal{M}} x_{m,\text{UE}}^{(\ell)}$, and the corresponding computing latency is

$$T_{\text{UE,cp}}^{(\ell)} = \frac{D_{\text{UE}}^{(\ell)} \phi}{C_{\text{UE}}}, \quad (1)$$

where ϕ is the expert computing workload (in FLOPs) for processing a hidden state and C_{UE} is the computation capability (in FLOP/s) of the user.

Accordingly, the total latency at MoE layer ℓ when activating local expert is given by

$$T_{\text{UE}}^{(\ell)} = I_{\text{UE}}^{(\ell)} T_{\text{UE,load}} + T_{\text{UE,cp}}^{(\ell)}. \quad (2)$$

Here, $I_{\text{UE}}^{(\ell)} = \mathbb{I}(D_{\text{UE}}^{(\ell)})$ is an indicator function, where $I_{\text{UE}}^{(\ell)} = 1$ only if $D_{\text{UE}}^{(\ell)} > 0$. Otherwise, $I_{\text{UE}}^{(\ell)} = 0$.

Let $P_{\text{UE,load}}$ denote the power of loading an expert at the user and $P_{\text{UE,cp}}$ denote the local computing power. Then, the energy consumption incurred by activating the local expert at layer ℓ is given by

$$E_{\text{UE}}^{(\ell)} = I_{\text{UE}}^{(\ell)} P_{\text{UE,load}} T_{\text{UE,load}} + P_{\text{UE,cp}} T_{\text{UE,cp}}^{(\ell)}. \quad (3)$$

B. Computation Offloading Model

We next consider the case where a token activates an expert at a helper $n \in \mathcal{N}$. In this case, the inference of each MoE layer consists of three stages: i) uplink transmission of the hidden state from the user to the helper, ii) expert loading and computation at the helper, and iii) downlink transmission of the output back to the user. Loading an expert into the helper n ’s GPU memory incurs an additional latency, denoted by $T_{n,\text{load}}$, which can be performed in parallel with the uplink transmission.

We assume the total bandwidth B assigned to the user is partitioned among the helpers, where B_n denotes the bandwidth allocated to helper n . After determining the activated expert(s) of each token, the user simultaneously uploads its hidden state to the helpers hosting those experts. Let $p_{\text{UE},n}^{(\ell)}$ denote the transmit power from the user to helper n . Then, the corresponding uplink achievable rate $R_{\text{UE},n}^{(\ell)}$ is given by

$$R_{\text{UE},n}^{(\ell)} = B_n \log_2 \left(1 + \frac{p_{\text{UE},n}^{(\ell)} d_n^{-\alpha} G_{\text{UE},n} h_n^{(\ell)}}{N_0 B_n} \right), \quad (4)$$

where d_n is the distance between the user and helper n , α is the path-loss factor, $G_{\text{UE},n}$ is the uplink antenna-related factor, N_0 is the noise power spectral density, and $h_n^{(\ell)}$ is the small-scale channel fading variable.

Similarly, after processing, the expert output should be downloaded from the helpers to the user. The downlink achievable rate $R_{n,\text{UE}}^{(\ell)}$ can be expressed as

$$R_{n,\text{UE}}^{(\ell)} = B_n \log_2 \left(1 + \frac{P_{n,\text{UE}} d_n^{-\alpha} G_{n,\text{UE}} h_n^{(\ell)}}{N_0 B_n} \right), \quad (5)$$

where $P_{n,\text{UE}}$ denotes the transmit power from helper n to the user and $G_{n,\text{UE}}$ is the downlink antenna-related factor.

Let $x_{m,n}^{(\ell)}$ denote a binary expert selection variable at the helpers, where $x_{m,n}^{(\ell)} = 1$ indicates that token m activates the expert at helper n in MoE layer ℓ , and $x_{m,n}^{(\ell)} = 0$ otherwise. Accordingly, the number of tokens processed by helper n at layer ℓ , denoted by $D_n^{(\ell)}$, is obtained by $D_n^{(\ell)} = \sum_{m \in \mathcal{M}} x_{m,n}^{(\ell)}$.

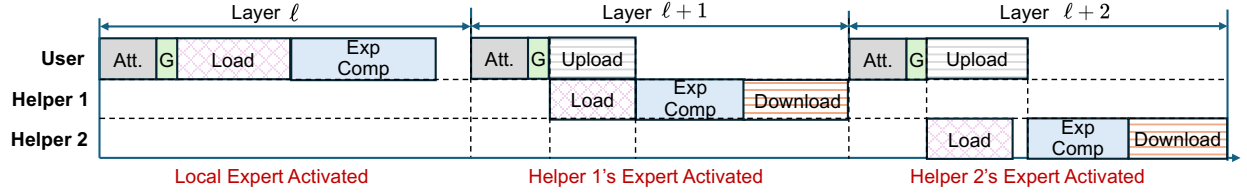


Fig. 2. Timeline of SiftMoE inference.

Therefore, the uplink and downlink transmission latency between the user and helper n for layer ℓ is calculated as

$$T_{\text{UE},n}^{(\ell)} = \frac{D_n^{(\ell)} b}{R_{\text{UE},n}^{(\ell)}}, \quad (6)$$

and

$$T_{n,\text{UE}}^{(\ell)} = \frac{D_n^{(\ell)} b}{R_{n,\text{UE}}^{(\ell)}}. \quad (7)$$

Moreover, expert processing latency at helper n during layer ℓ is given by

$$T_{n,\text{cp}}^{(\ell)} = \frac{D_n^{(\ell)} \phi}{C_n}, \quad (8)$$

where C_n is the computation capability (in FLOP/s) of helper n . Therefore, the total latency incurred by activating the expert at helper n during MoE layer ℓ is given by

$$T_n^{(\ell)} = \max \left\{ T_{\text{UE},n}^{(\ell)}, T_{n,\text{load}}^{(\ell)} \right\} + T_{n,\text{cp}}^{(\ell)} + T_{n,\text{UE}}^{(\ell)}. \quad (9)$$

By combining (4) and (6), the transmission energy consumption from the user to helper n for MoE layer ℓ , denoted by $E_n^{(\ell)}$, is given by

$$E_n^{(\ell)} = p_{\text{UE},n}^{(\ell)} T_{\text{UE},n}^{(\ell)} = \frac{\left(2^{\frac{D_n^{(\ell)} b}{B_n T_{\text{UE},n}^{(\ell)}}} - 1 \right) N_0 B_n T_{\text{UE},n}^{(\ell)}}{d_n^{-\alpha} G_{\text{UE},n} h_n^{(\ell)}}. \quad (10)$$

We ignore the receiving power consumption at the user because it is often much smaller than the transmit power [32]–[34].

III. ERROR ANALYSIS OF EXPERT SELECTION

In this section, we first provide a theoretical analysis of the per-layer error caused by expert selection. We then derive the allowable error at each MoE layer under a constraint on the final output deviation. These results lay the analytical foundation for the energy-efficient expert selection design developed in Sections IV and V.

A. Preliminaries and Assumptions

Consider an input token representation $z \in \mathbb{R}^d$, where d denotes the hidden-state dimension. At each MoE layer, the gating network computes a vector of routing logits given by $\mathcal{P}(z) = \mathbf{W}_r^T z$, where $\mathbf{W}_r \in \mathbb{R}^{d \times N}$ is the router matrix. Based on the routing logits, an expert activation set \mathcal{A} is selected. Thus, the output of the MoE layer can be expressed as $y(z) = \sum_{i \in \mathcal{A}} g_i(z) \text{FFN}_i(z)$, where $\text{FFN}_i(z)$ is the output result of

expert i and $g_i(z) = \frac{\exp(\mathcal{P}_i(z))}{\sum_{i' \in \mathcal{A}} \exp(\mathcal{P}_{i'}(z))}$ denotes the softmax-normalized gating score associated with expert i .

Each expert is implemented as an FFN, which is a standard neural network architecture. Therefore, we adopt the following assumptions commonly used in the theoretical analysis of deep neural networks.

Assumption 1. (Bounded expert outputs) [35] For the ℓ -th MoE layer, the outputs of expert networks are assumed to be uniformly bounded over \mathcal{Z} , i.e., $\|\text{FFN}_i^{(\ell)}(z)\|_2 \leq B_{\max}^{(\ell)}$ for $z \in \mathcal{Z}$ and $i \in \mathcal{E}^{(\ell)}$.

Assumption 2. (Lipschitz continuity of experts) [36], [37] For the ℓ -th MoE layer, each expert network $\text{FFN}_i^{(\ell)}(\cdot)$ is assumed to be $\beta_{\mathcal{E},i}^{(\ell)}$ -Lipschitz continuous over \mathcal{Z} , i.e., $\|\text{FFN}_i^{(\ell)}(\tilde{z}) - \text{FFN}_i^{(\ell)}(z)\|_2 \leq \beta_{\mathcal{E},i}^{(\ell)} \|\tilde{z} - z\|_2$ for $z, \tilde{z} \in \mathcal{Z}$ and $i \in \mathcal{E}^{(\ell)}$.

B. Effect of Expert Selection on Output Results

Consider MoE layer ℓ . Let $\mathcal{A}_{\text{Top}}^{(\ell)}(z)$ denote the set of activated expert(s) at layer ℓ with an input hidden state z under traditional Top- K selection strategy. The resulting output representation at this layer under the Top- K scheme is given by

$$y_{\text{Top}}^{(\ell)}(z) = \sum_{i \in \mathcal{A}_{\text{Top}}^{(\ell)}(z)} g_i^{(\ell)}(z) \text{FFN}_i^{(\ell)}(z), \quad (11)$$

where $g_i^{(\ell)}(z)$ denotes the gating score associated with expert i at layer ℓ .

When resource-aware expert selection is applied, the resulting activated expert set is denoted by $\tilde{\mathcal{A}}^{(\ell)}(z)$. In this case, the layer output becomes

$$\tilde{y}^{(\ell)}(z) = \sum_{i \in \tilde{\mathcal{A}}_{\text{Top}}^{(\ell)}(z)} g_i^{(\ell)}(z) \text{FFN}_{\varphi(i)}^{(\ell)}(z). \quad (12)$$

Here, for any expert $i \in \tilde{\mathcal{A}}_{\text{Top}}^{(\ell)}(z)$, $\varphi(i)$ denotes the expert actually used under the resource-aware expert selection scheme. If $\varphi(i) = i$, expert i is retained. If $\varphi(i) \neq i$ and $\varphi(i) \neq \emptyset$, then $\varphi(i)$ is a substitute expert for i . Otherwise, $\varphi(i) = \emptyset$, indicating that expert i is skipped.

Define the deviation by expert selection at layer ℓ with input z as $\delta^{(\ell)}(z) \triangleq \|\tilde{y}^{(\ell)}(z) - y_{\text{Top}}^{(\ell)}(z)\|_2$. The following proposition establishes an upper bound on the expected deviation at each MoE layer.

Proposition 1 (Expected layer-wise deviation). With expert selection, the expected deviation at MoE layer ℓ satisfies

$$\mathbb{E} \left[\delta^{(\ell)}(z) \right] \leq \sum_{i \in \mathcal{A}_{\text{Top}}^{(\ell)}(z)} g_i^{(\ell)}(z) \mathbb{E} \left[F_{i, \varphi(i)}^{(\ell)}(z) \right], \quad (13)$$

where $F_{i, \varphi(i)}^{(\ell)}(z) \triangleq \frac{\left\| \text{FFN}_i^{(\ell)}(z) \right\|_2}{\sqrt{1 + \rho_{i, \varphi(i)}^{(\ell)}(z)^2 - 2\rho_{i, \varphi(i)}^{(\ell)}(z) \cos \theta_{i, \varphi(i)}^{(\ell)}(z)}}$. Here, $\rho_{i, \varphi(i)}^{(\ell)}(z) = \frac{\left\| \text{FFN}_{\varphi(i)}^{(\ell)}(z) \right\|_2}{\left\| \text{FFN}_i^{(\ell)}(z) \right\|_2}$ is the ratio between the output norms of experts i and $\varphi(i)$, and $\cos \theta_{i, \varphi(i)}^{(\ell)}(z) = \frac{\text{FFN}_i^{(\ell)}(z) \cdot \text{FFN}_{\varphi(i)}^{(\ell)}(z)}{\left\| \text{FFN}_i^{(\ell)}(z) \right\|_2 \left\| \text{FFN}_{\varphi(i)}^{(\ell)}(z) \right\|_2}$ denotes the cosine similarity between their output vectors.

Proof. Please see Appendix A. \square

Proposition 1 indicates that experts with small gating scores contribute marginally to the aggregated output. Consequently, replacing or skipping such experts only induces a marginal change in the expected deviation. In contrast, experts with large gating scores play a dominant role in the layer output. Therefore, substituting a high-score expert requires selecting a functionally similar alternative. Otherwise, a large discrepancy between expert outputs may occur, thereby increasing the resulting layer-wise deviation.

Remark 1 (Skipping versus replacement). Skipping an expert can be equivalently interpreted as replacing it with a null expert whose output is the zero vector, and the deviation caused by skipping expert i in layer ℓ is $g_i^{(\ell)}(z) \left\| \text{FFN}_i^{(\ell)}(z) \right\|_2$. On the other hand, replacing expert i with an alternative \tilde{i} introduces a deviation scaled by the mismatch factor $\frac{1}{\sqrt{1 + \rho_{i, \tilde{i}}^{(\ell)}(z)^2 - 2\rho_{i, \tilde{i}}^{(\ell)}(z) \cos \theta_{i, \tilde{i}}^{(\ell)}(z)}}$. When this factor exceeds one, the deviation induced by replacement is strictly larger than that caused by skipping. Such a regime naturally arises when the substitute expert is functionally dissimilar to the original one. Consequently, skipping a low-impact expert may perform better than replacing it with a poorly matched alternative.

We next characterize how per-layer deviations induced by expert selection accumulate across layers and affect the final model output. Let $e^{(\ell)} = \left\| \tilde{y}^{(\ell)} - y_{\text{Top}}^{(\ell)} \right\|_2$ denote the output deviation at layer ℓ with the initialization $e^{(0)} = 0$, which captures the *accumulated deviation* between the expert-selection output and the corresponding Top- K output up to layer ℓ .

Theorem 1 (Final output deviation bound). Given an expert selection scheme, there is an upper bound on the accumulated deviation of the model output space:

$$e^{(\ell)} \leq \sum_{r=1}^{\ell} \left[\left(2B_{\max}^{(r)} + \delta^{(r)} \right) \prod_{t=r+1}^{\ell} \beta_{\text{E,max}}^{(t)} \right], \quad (14)$$

where $\beta_{\text{E,max}}^{(\ell)} = \max_{i \in \mathcal{E}^{(\ell)}} \beta_{\text{E},i}^{(\ell)}$.

Proof. Please see Appendix B. \square

Theorem 1 provides several insights into how layer-wise expert selection errors propagate across MoE layers. First, the final output deviation is determined by the cumulative effect of deviations introduced at all preceding layers, indicating that expert-selection errors are inherently cross-layer coupled. Second, the product term $\prod_{t=r+1}^{\ell} \beta_{\text{E,max}}^{(t)}$ shows that deviations introduced at earlier layers may be amplified by subsequent layers, making shallow-layer errors generally more critical than those in deeper layers. Third, by separating the layer-wise selection error $\delta^{(r)}$ from the model-dependent constants $\beta_{\text{E,max}}^{(\ell)}$ and $B_{\max}^{(\ell)}$, the bound reveals that different layers can tolerate different levels of deviation depending on their error amplification effects. Therefore, this result establishes a direct link between local expert-selection deviations and the final output deviation, enabling global accuracy requirements to be translated into tractable layer-wise constraints for the subsequent expert selection design.

Based on Theorem 1, we next characterize how the expected layer-wise deviation induced by expert selection should be controlled in order to guarantee a target expected output accuracy.

Corollary 1 (Expected per-layer deviation budget). Assuming that the expected intermediate deviation satisfies $\mathbb{E}[e^{(\ell)}] \leq \kappa^{(\ell)}$ for $\ell = 1, \dots, L-1$, and the final deviation satisfies $\mathbb{E}[e^{(L)}] \leq \theta$ with a nonnegative allocation $\{\theta^{(\ell)}\}_{\ell=1}^L$ such that $\sum_{\ell=1}^L \theta^{(\ell)} = \theta$. Then, the expected deviation induced by expert selection at MoE layer ℓ must satisfy

$$\mathbb{E} \left[\delta^{(\ell)} \right] \leq \eta^{(\ell)}, \quad (15)$$

where $\eta^{(\ell)} = \min \left\{ \kappa^{(\ell)} - 2B_{\max}^{(\ell)} - \sum_{r=1}^{\ell-1} f(r, \ell), \frac{\theta^{(\ell)}}{\prod_{t=\ell+1}^L \beta_{\text{E,max}}^{(t)}} - 2B_{\max}^{(\ell)} \right\}$ and $f(r, \ell) = \frac{1}{\left(2B_{\max}^{(r)} + \delta^{(r)} \right) \prod_{t=r+1}^{\ell} \beta_{\text{E,max}}^{(t)}}$.

IV. EXPERT SELECTION UNDER SLOW FADING

In this section, we formulate an optimization problem for energy-efficient expert selection under slow-fading channels, leveraging the allowable per-layer deviations derived in Section III to enforce accuracy constraints. Under slow-fading channels, the small-scale fading coefficients may vary across different MoE layers but remain constant within each layer. We first study the decoding phase, where a single token is processed and the optimal solution admits a simple structure. Then, we extend the analysis to the multi-token prefilling phase. The fast-fading scenario will be discussed in Section V.

A. Problem Formulation

Our objective is to minimize the total energy consumption across all MoE layers by optimizing the expert selection decisions during inference. Let $\mathbf{X}^{(\ell)} = \left\{ x_{m,v}^{(\ell)} \right\}_{m \in \mathcal{M}, v \in \mathcal{V}}$ denote the binary expert selection variables at MoE layer ℓ . Due to the sequential nature of MoE inference, the gating scores and expert activation information are revealed layer by

layer, preventing us from solving the problem for the whole MoE model. Moreover, the energy consumption, as well as the latency and accuracy constraints, can be layer-wise separable if we introduce an accuracy budget for each layer according to Corollary 1. Therefore, to minimize the total energy, we focus on minimizing energy for each layer:

$$\mathcal{P}1: \quad \min_{\mathbf{X}^{(\ell)}} E^{(\ell)} = E_{\text{UE}}^{(\ell)} + \sum_{n \in \mathcal{N}} E_n^{(\ell)} \quad (16a)$$

$$\text{s.t.} \quad T_v^{(\ell)} \leq T, \forall v \in \mathcal{V}, \quad (16b)$$

$$\mathbb{E} \left[\left\| \delta^{(\ell)}(z_m) \right\|_2 \right] \leq \eta^{(\ell)}, \forall m \in \mathcal{M}, \quad (16c)$$

$$1 \leq \sum_{v \in \mathcal{V}} x_{m,v}^{(\ell)} \leq K, \forall m \in \mathcal{M}, \quad (16d)$$

$$x_{m,v}^{(\ell)} \in \{0, 1\}, \forall m \in \mathcal{M}, v \in \mathcal{V}, \quad (16e)$$

where Constraint (16b) ensures that the latency of each layer does not exceed a threshold T . Constraint (16c) limits the inference accuracy degradation caused by expert selection at each MoE layer. Constraint (16d) restricts the number of experts activated by each token to at most K , ensuring fairness and comparability with the conventional Top- K routing scheme. Constraint (16e) denotes that the expert selection variable is a binary one.

B. Decoding Phase with a Single Token

During the decoding phase, only a single token is processed at each step of autoregressive inference. In this scenario, the token index m can be omitted for simplicity. The resulting optimization problem admits a simplified structure and a more tractable solution. Accordingly, the energy consumption of local computing can be expressed as

$$\bar{E}_{\text{UE}}^{(\ell)} = x_{\text{UE}}^{(\ell)} \left(P_{\text{UE,load}} T_{\text{UE,load}} + \frac{P_{\text{UE,cp}} \phi}{C_{\text{UE}}} \right). \quad (17)$$

For helper-side processing, we notice that $E_n^{(\ell)}$ is a non-increasing function related to $T_{\text{UE},n}^{(\ell)}$. Thus, the uplink transmission time $T_{\text{UE},n}^{(\ell)}$ should be maximized if the expert at helper n is activated, and the optimal total latency at helper n is $T_n^{(\ell)*} = x_n^{(\ell)} T$. By jointly considering constraints (16b) and (16c), we define the feasible set $\Omega^{(\ell)}$ as the collection of edge-node subsets, where each subset consists of at most K edge nodes hosting experts that satisfy the latency and accuracy constraints. Then, the optimal uplink transmission energy from the user to helper $n \in \Omega^{(\ell)}$ is given by

$$\bar{E}_n^{(\ell)} = x_n^{(\ell)} \frac{\left(2^{\frac{b}{B_n \bar{T}_{\text{UE},n}^{(\ell)}}} - 1 \right) N_0 B_n \bar{T}_{\text{UE},n}^{(\ell)}}{d_n^{-\alpha} G_{\text{UE},n} h_n^{(\ell)}}. \quad (18)$$

where $\bar{T}_{\text{UE},n}^{(\ell)} = T - \left(\frac{\phi}{C_n} + \frac{b}{R_{n,\text{UE}}^{(\ell)}} \right)$ denotes the remaining time budget for uplink transmission.

Based on the above analysis, the following theorem characterizes the optimal solution to problem $\mathcal{P}1$ under the single-token decoding case.

Theorem 2. Under the single-token decoding scenario, the optimal solution to problem $\mathcal{P}1$ at layer ℓ is expressed as

$$x_v^{(\ell)*} = \begin{cases} 1, & v \in \mathcal{J}^{(\ell)*}, \\ 0, & \text{otherwise.} \end{cases} \quad (19)$$

where

$$\mathcal{J}^{(\ell)*} = \arg \min_{\mathcal{J}^{(\ell)} \in \Omega^{(\ell)}} \sum_{v \in \mathcal{J}^{(\ell)}} f_v^{(\ell)}, \quad (20)$$

with $f_v^{(\ell)}$ being the energy cost at layer ℓ associated with selecting the expert hosted at edge node v , given by

$$f_v^{(\ell)} = \begin{cases} P_{v,\text{load}} T_{v,\text{load}} + \frac{P_{v,\text{cp}} \phi}{C_v}, & \text{if } v = \text{UE}, \\ \frac{\left(2^{\frac{b}{B_v \bar{T}_{\text{UE},v}^{(\ell)}}} - 1 \right) N_0 B_v \bar{T}_{\text{UE},v}^{(\ell)}}{d_v^{-\alpha} G_{\text{UE},v} h_v^{(\ell)}}, & \text{if } v \in \mathcal{N}. \end{cases} \quad (21)$$

Proof. The proof is straightforward and is omitted due to space limitations. \square

Remark 2. Consider the case $K = 1$, where each token activates only one expert at each layer. In this case, the feasible set $\Omega^{(\ell)}$ reduces to a set of individual edge nodes whose hosted experts satisfy the latency and accuracy constraints. Consequently, $\mathcal{P}1$ admits a closed-form solution: the optimal expert is the one associated with the minimum per-expert energy cost $f_v^{(\ell)}$ among all feasible candidates. That is, the optimal decision is obtained by selecting $v^* = \arg \min_{v \in \Omega^{(\ell)}} f_v^{(\ell)}$, and setting $x_{v^*}^{(\ell)} = 1$ and $x_v^{(\ell)} = 0$ for all $v \neq v^*$.

C. Prefilling Phase with Multiple Tokens

In this subsection, we consider the prefill phase where multiple input tokens are processed simultaneously. Unlike the decoding phase where only a single token is processed, tokens compete for the resources of the same helper. Therefore, expert selection decisions must be jointly optimized across tokens.

Each token may be offloaded to one or more helpers, which is governed by K . When $K = 1$, each token is assigned to exactly one helper, and the resulting optimization problem reduces to a one-to-many assignment. When $K > 1$, each token selects a subset of helpers, and the feasible decisions are defined over combinations of helpers rather than individual nodes. This introduces additional combinatorial coupling among helpers within each token's decision. Consequently, the structure of the optimization problem with $K > 1$ is fundamentally different from that with $K = 1$, and the algorithm designed for the $K = 1$ case cannot be directly applied. We therefore distinguish these two settings and analyze them separately: we first consider the case with $K = 1$, and then study the case with $K \geq 1$.

1) *When $K = 1$:* Recall that $E_n^{(\ell)}$ is a non-increasing function of $T_{\text{UE},n}^{(\ell)}$. Therefore, the uplink transmission time $T_{\text{UE},n}^{(\ell)}$ should be maximized. When $I_n^{(\ell)} > 0$, the optimal uplink transmission latency is given by $T_{\text{UE},n}^{(\ell)*} = T - D_n^{(\ell)} \left(\frac{\phi}{C_n} + \frac{b}{R_{n,\text{UE}}^{(\ell)}} \right)$. Otherwise, $T_{\text{UE},n}^{(\ell)*} = 0$. Therefore, the optimal uplink energy consumption of transmitting hidden states to helper n can be given by $\bar{E}_n^{(\ell)*} =$

$\left(\frac{D_n^{(\ell)} b}{2^{B_n T_{UE,n}^{(\ell)*}} - 1} \right) N_0 B_n T_{UE,n}^{(\ell)*}$. In particular, when $D_n^{(\ell)} = 0$, $E_n^{(\ell)*} = 0$ holds.

With the above optimal transmission strategy for any given load, we now analyze the properties of the energy cost function to facilitate the token-to-helper assignment.

Proposition 2. $E_{UE}^{(\ell)}$ is a monotonically increasing and discretely linear function of $D_{UE}^{(\ell)}$, and $E_n^{(\ell)}$ is a monotonically increasing and discretely convex function of $D_n^{(\ell)}$.

Proof. Please see Appendix C. \square

From Proposition 2, the following analysis focuses on $E_n^{(\ell)}$, which exhibits a nonuniform marginal-cost structure. The term $E_{UE}^{(\ell)}$ corresponds to the constant marginal-cost case and can be treated as a special case. Define the marginal cost of assigning the d -th token to helper n as $\Delta E_n^{(\ell)}(d) \triangleq E_n^{(\ell)}(d) - E_n^{(\ell)}(d-1)$. Since $E_n^{(\ell)}$ is discretely convex in $D_n^{(\ell)}$, the marginal cost sequence $\{\Delta E_n^{(\ell)}(d)\}$ is nondecreasing in d . Accordingly, the energy cost of transmitting to helper n can be expressed as an accumulated sum of marginal costs, i.e., $E_n^{(\ell)}(D_n^{(\ell)}) = \sum_{d=1}^{D_n^{(\ell)}} \Delta E_n^{(\ell)}(d)$. This decomposition admits an exact slot-based interpretation: assigning $D_n^{(\ell)}$ tokens to helper n is equivalent to occupying the first $D_n^{(\ell)}$ unit-capacity slots, where occupying the d -th slot incurs a cost $\Delta E_n^{(\ell)}(d)$. Due to the monotonicity of the marginal costs, any feasible assignment that occupies a higher-index slot while leaving a lower-index slot unused can be transformed into another feasible assignment with no higher cost by exchanging these slots. Repeating this exchange yields an optimal assignment whose occupied slots form a prefix $\{1, \dots, D_n^{(\ell)}\}$ for each helper. Hence, the slot representation constitutes an exact reformulation of the original discrete-convex objective.

When $K = 1$, each feasible combination in $\Omega_m^{(\ell)}$ contains a single helper. Under the exact slot-based reformulation, the token-expert matching problem can be cast as a linear min-cost flow problem and solved optimally using a successive shortest augmenting path (SSAP) algorithm [38]. Algorithm 1 implements this procedure without constructing all slot nodes. Specifically, we construct a residual network consisting of a source node s , token nodes $\{u_m\}_{m \in \mathcal{M}}$, expert nodes $\{q_v\}_{v \in \mathcal{V}}$, and a sink node t . Edges $s \rightarrow u_m$ represent the initiation of token assignments, while edges $q_v \rightarrow t$ capture the marginal energy cost incurred when assigning additional tokens to node q_v . All arcs have unit capacity unless otherwise specified. Under the discrete-convex objective, any load-preserving reassignment corresponds to a zero-cost cycle in the residual network. Augmenting flow along such cycles enables the SSAP algorithm to revise earlier assignments without increasing the total cost.

The optimality of Algorithm 1 follows from standard results on minimum-cost flow, where the SSAP algorithm is guaranteed to find a globally optimal solution [38]. Since the graph may contain negative weights, the Bellman-Ford algorithm can be adopted to find the shortest path. Fol-

Algorithm 1 Successive shortest augmenting path-based token-expert matching when $K = 1$

```

1: Input: Token set  $\mathcal{M}$ , edge node set  $\mathcal{V}$ , computing capacity
   limits  $\{D_{v,\max}^{(\ell)}\}_{v \in \mathcal{V}}$ ; feasible sets  $\{\Omega_m^{(\ell)}\}_{m \in \mathcal{M}}$ ; marginal
   energy costs  $\{\Delta E_v(d)\}_{v \in \mathcal{V}, d \leq D_{v,\max}^{(\ell)}}$ .
2: Initialize  $D_v^{(\ell)} \leftarrow 0, \forall v \in \mathcal{V}$ ,  $x_{m,v}^{(\ell)} \leftarrow 0$  for all admissible
    $(m, v)$ , and total required flow  $F \leftarrow |\mathcal{M}|$ .
3: while  $F > 0$  do
4:   Construct a residual network  $\mathcal{G}_{\text{res}}$  with nodes  $\{s\} \cup$ 
    $\{u_m\}_{m \in \mathcal{M}} \cup \{q_v\}_{v \in \mathcal{V}} \cup \{t\}$ .
5:   for each token  $m \in \mathcal{M}$  do
6:     if  $\sum_{v \in \Omega_m^{(\ell)}} x_{m,v}^{(\ell)} = 0$  then
7:       Add arc  $(s \rightarrow u_m)$  with cost 0.
8:     else
9:       Add arc  $(u_m \rightarrow s)$  with cost 0.
10:    end if
11:   end for
12:   for each admissible pair  $(m, v)$  with  $v \in \Omega_m^{(\ell)}$  do
13:     if  $x_{m,v}^{(\ell)} = 0$  then
14:       Add arc  $(u_m \rightarrow q_v)$  with cost 0.
15:     else
16:       Add arc  $(q_v \rightarrow u_m)$  with cost 0.
17:     end if
18:   end for
19:   for each edge node  $v \in \mathcal{V}$  do
20:     if  $D_v^{(\ell)} < D_{v,\max}^{(\ell)}$  then
21:       Add arc  $(q_v \rightarrow t)$  with cost  $\Delta E_v(D_v^{(\ell)} + 1)$ .
22:     end if
23:     if  $D_v^{(\ell)} > 0$  then
24:       Add arc  $(t \rightarrow q_v)$  with cost  $-\Delta E_v(D_v^{(\ell)})$ .
25:     end if
26:   end for
27:   Find a shortest path  $P$  from  $s$  to  $t$  in  $\mathcal{G}_{\text{res}}$  using
   Bellman-Ford algorithm. If no such path exists, terminate
   and declare the problem infeasible. Otherwise, augment
   one unit of flow along  $P$ .
28:   for each arc  $(a \rightarrow b)$  on path  $P$  do
29:     if  $(a \rightarrow b) = (u_m \rightarrow q_v)$  then
30:        $x_{m,v}^{(\ell)} \leftarrow 1, D_v^{(\ell)} \leftarrow D_v^{(\ell)} + 1$ .
31:     else if  $(a \rightarrow b) = (q_v \rightarrow u_m)$  then
32:        $x_{m,v}^{(\ell)} \leftarrow 0, D_v^{(\ell)} \leftarrow D_v^{(\ell)} - 1$ .
33:     end if
34:   end for
35:    $F \leftarrow F - 1$ .
36: end while
37: return  $\{x_{m,v}^{(\ell)}\}$ .

```

lowing standard complexity results for the SSAP algorithm [38], the computational complexity of Algorithm 1 is $\mathcal{O}\left(M(M+N)\left(M+N+\sum_{m \in \mathcal{M}} |\Omega_m^{(\ell)}|\right)\right)$.

2) When $K \geq 1$: When each token can be assigned to multiple edge nodes, i.e., $K > 1$, the structure of $\mathcal{P}1$ fundamentally changes. The feasible decision for each token is no longer a single edge node but a combination of edge nodes, which introduces combinatorial coupling across selection vari-

ables. As a result, $\mathcal{P}1$ becomes NP-hard. Nevertheless, two structural properties enable efficient algorithm design. First, the marginal cost formulation derived for the $K = 1$ case still applies. Second, the system evolves sequentially across tokens and can be characterized by the helper load vector, which naturally leads to a load-based system state.

These structural properties motivate a DP formulation. By representing the system state using the helper load vector, the problem can be modeled as a sequential decision process across tokens. Accordingly, we develop a DP-based algorithm that yields the globally optimal solution for moderate problem sizes, as shown in Algorithm 2. Specifically, each token $m \in \mathcal{M}$ selects exactly one feasible edge node combination $J_m^{(\ell)} \in \Omega_m^{(\ell)}$, where each combination satisfies $1 \leq |J_m^{(\ell)}| \leq K$. For token m , let $\text{DP}_m^{(\ell)}(\mathbf{D})$ denote the minimum total energy incurred by the first m tokens, given the current load vector over all edge nodes $\mathbf{D} = \{D_v^{(\ell)}\}_{v \in \mathcal{V}}$. When token m selects a combination $J_m^{(\ell)}$, the system transitions to a successor state $\tilde{\mathbf{D}} = \{\tilde{D}_v^{(\ell)}\}_{v \in \mathcal{V}}$, where the load of each edge node v is incremented by one. By iterating over tokens and feasible combinations, the DP algorithm explores all admissible load evolutions.

The optimality of Algorithm 2 follows from Bellman's principle of optimality, as the problem exhibits an optimal substructure and the DP formulation exhaustively explores all feasible state transitions [39]. Following standard DP procedure [39], it is easy to show that the upper bound on the computational complexity of Algorithm 2 is $\mathcal{O}\left(M\Omega_{\max}K \prod_n (D_{n,\max}^{(\ell)} + 1)\right)$, where $\Omega_{\max} = \max_{m \in \mathcal{M}} |\Omega_m^{(\ell)}|$. Note that Algorithm 2 also applies to the case $K = 1$. However, for $K = 1$, the problem admits a simpler structure and can be solved more efficiently by Algorithm 1.

3) *Design insights*: The following remarks provide insight into the structural reasons behind the optimality of the proposed algorithms for arbitrary K and characterize the optimal transmission strategy.

Remark 3 (Marginal-cost curvature over feasible edge loads). The optimal token-expert assignment is governed entirely by the growth rate of the marginal energy cost with respect to edge load. For helper nodes, the discretely convex uplink energy function induces a load-dependent marginal cost whose curvature determines the assignment behavior. When the marginal cost increases steeply due to limited computing capability, unfavorable user-helper channel conditions, or tight transmission time constraints, assigning many tokens to the same helper becomes energy-inefficient, and tokens are preferentially assigned to other helpers with lower marginal costs. Conversely, when the marginal cost grows slowly over the feasible load region, additional tokens tend to be assigned to that helper until its marginal cost becomes comparable to others. The user (local computing) corresponds to a special linear case with constant marginal cost.

Remark 4 (Cost symmetry and non-uniqueness). The system cost depends only on the edge node's load vector $D_v^{(\ell)}$ and

Algorithm 2 DP-based token-expert matching when $K \geq 1$

- 1: **Input**: Token set \mathcal{M} , edge node set \mathcal{V} , computing capacity limits $\{D_{v,\max}^{(\ell)}\}_{v \in \mathcal{V}}$; feasible sets $\{\Omega_m^{(\ell)}\}_{m \in \mathcal{M}}$; marginal energy costs $\{\Delta E_v(d)\}_{v \in \mathcal{V}, d \leq D_{v,\max}^{(\ell)}}$.
 - 2: Initialize DP table: $\text{DP}_0^{(\ell)}(\mathbf{D}) \leftarrow +\infty$ for all states \mathbf{D} , and $\text{DP}_0^{(\ell)}(\mathbf{0}) \leftarrow 0$, where $\mathbf{D} = \{D_v^{(\ell)}\}_{v \in \mathcal{V}}$.
 - 3: Initialize backtracking pointers: $\text{ParState}_0^{(\ell)}(\mathbf{0}) \leftarrow \emptyset$, $\text{ParComb}_0^{(\ell)}(\mathbf{0}) \leftarrow \emptyset$.
 - 4: **for** $m = 1$ to M **do**
 - 5: Initialize $\text{DP}_m^{(\ell)}(\mathbf{D}) \leftarrow +\infty$ for all states \mathbf{D} .
 - 6: **for** each state \mathbf{D} with $\text{DP}_{m-1}^{(\ell)}(\mathbf{D}) < +\infty$ **do**
 - 7: **for** each combination $J \in \Omega_m^{(\ell)}$ **do**
 - 8: **if** $D_v^{(\ell)} + 1 \leq D_{v,\max}^{(\ell)}$ for all $v \in J$ **then**
 - 9: **for** each edge node $v \in \mathcal{V}$ **do**
 - 10: **if** $v \in J$ **then**
 - 11: $\tilde{D}_v^{(\ell)} \leftarrow D_v^{(\ell)} + 1$
 - 12: **else**
 - 13: $\tilde{D}_v^{(\ell)} \leftarrow D_v^{(\ell)}$
 - 14: **end if**
 - 15: **end for**
 - 16: $\Delta \leftarrow \sum_{v \in J} \Delta E_v(D_v^{(\ell)} + 1)$.
 - 17: **if** $\text{DP}_{m-1}^{(\ell)}(\mathbf{D}) + \Delta < \text{DP}_m^{(\ell)}(\tilde{\mathbf{D}})$ **then**
 - 18: $\text{DP}_m^{(\ell)}(\tilde{\mathbf{D}}) \leftarrow \text{DP}_{m-1}^{(\ell)}(\mathbf{D}) + \Delta$;
 - 19: $\text{ParState}_m^{(\ell)}(\tilde{\mathbf{D}}) \leftarrow \mathbf{D}$; $\text{ParComb}_m^{(\ell)}(\tilde{\mathbf{D}}) \leftarrow J$.
 - 20: **end if**
 - 21: **end for**
 - 22: **end for**
 - 23: **end for**
 - 24: Select terminal state: $\mathbf{D}^* \leftarrow \arg \min_{\mathbf{D}} \text{DP}_M^{(\ell)}(\mathbf{D})$. Backtracking to recover $\{J_m^{(\ell)*}\}$: $\mathbf{D}_{\text{cur}} \leftarrow \mathbf{D}^*$.
 - 25: **for** $m = M$ down to 1 **do**
 - 26: $J_m^{(\ell)*} \leftarrow \text{ParComb}_m^{(\ell)}(\mathbf{D}_{\text{cur}})$. $\mathbf{D}_{\text{cur}} \leftarrow \text{ParState}_m^{(\ell)}(\mathbf{D}_{\text{cur}})$.
 - 27: **end for**
 - 28: **return** Optimal expert subset selection $\{J_m^{(\ell)*}\}$.
-

is invariant to the identities of individual tokens. This load-based symmetry implies that tokens with nested feasible edge node sets can be reassigned or exchanged across edge nodes without violating DP optimality, as long as the resulting load vector remains unchanged.

Remark 5 (Uniform bit transmission under slow fading). Under slow fading, the uplink transmission energy is a convex function of the number of transmitted bits over the layer duration. Therefore, for a given uplink transmission time budget, evenly distributing the required bits across time slots minimizes the total energy consumption.

V. JOINT EXPERT SELECTION AND ADAPTIVE TRANSMISSION UNDER FAST FADING

In contrast to the slow-fading case discussed in Section IV, fast fading introduces time-varying channel conditions within

each MoE layer. Under such dynamics, uniformly distributing transmitted bits (in Remark 5) across time slots is no longer energy-optimal, and exploiting channel variations through adaptive slot-level bit allocation becomes necessary. In this section, we study the joint optimization of expert selection and per-slot bit allocation under fast fading to minimize expected energy consumption.

A. Problem Reformulation

To model fast fading within each MoE layer, we partition the uplink transmission phase into multiple time slots of equal duration τ . The channel gain is assumed to be quasi-static, i.e., being constant within each slot but varying independently across slots. Accordingly, the uplink transmission energy incurred by helper n in time slot t of MoE layer ℓ is given by

$$E_{n,t}^{(\ell)} = \frac{\left(2^{\frac{\gamma_{n,t}^{(\ell)}}{B_n \tau}} - 1\right) N_0 B_n \tau}{d_n^{-\alpha} G_{\text{UE},n} h_{n,t}^{(\ell)}}, \quad (22)$$

where $\gamma_{n,t}^{(\ell)}$ is the number of bits transmitted from the user to helper n in slot t of layer ℓ , and $h_{n,t}^{(\ell)}$ is the corresponding fast-fading channel gain.

We now formulate the joint optimization of expert selection $\mathbf{X}^{(\ell)}$ and slot-level bit allocation $\gamma^{(\ell)}$ under fast fading. Specifically, for each MoE layer ℓ , the problem is given by

$$\mathcal{P}2: \quad \min_{\mathbf{X}^{(\ell)}, \gamma^{(\ell)}} E_{\text{UE}}^{(\ell)} + \mathbb{E}_h \left[\sum_{n \in \mathcal{N}} \sum_{t=1}^{Q_n^{(\ell)}} E_{n,t}^{(\ell)} \right] \quad (23a)$$

$$\text{s.t.} \quad (16b) - (16e), \quad (23b)$$

$$\sum_{t=1}^{Q_n^{(\ell)}} \gamma_{n,t}^{(\ell)} = b D_n^{(\ell)}, \forall n \in \mathcal{N}, \ell \in \mathcal{L}, \quad (23c)$$

where $Q_n^{(\ell)} = \left\lceil \frac{T_{\text{UE},n}^{(\ell)}}{\tau} \right\rceil$ denotes the number of uplink transmission slots allocated to helper n in layer ℓ .

Due to the separable sum-bit constraint across helpers, the inner optimization over $\gamma^{(\ell)}$ can be decomposed. Then, the total energy consumption of helpers in (23a) can be equivalently rewritten as

$$\min_{\mathbf{X}^{(\ell)}, \gamma^{(\ell)}} \mathbb{E}_h \left[\sum_{n \in \mathcal{N}} \sum_{t=1}^{Q_n^{(\ell)}} E_{n,t}^{(\ell)} \right] = \min_{\mathbf{X}^{(\ell)}} \sum_{n \in \mathcal{N}} E_n^{(\ell)*} \left(D_n^{(\ell)} \right),$$

where $E_n^{(\ell)*} \left(D_n^{(\ell)} \right) \triangleq \min_{\pi_n} \mathbb{E} \left[\sum_{t=1}^{Q_n^{(\ell)}} E_{n,t}^{(\ell)} \left(\gamma_{n,t}^{(\ell)}, h_{n,t}^{(\ell)} \right) \right]$ is the minimum expected uplink energy required to transmit $b D_n^{(\ell)}$ bits to helper n under fast fading, and π_n represents a causal bit-allocation policy that adapts $\gamma_{n,t}^{(\ell)}$ to the instantaneous fading $h_{n,t}^{(\ell)}$.

B. Expert Selection Scheme

Although exact, the value function $E_n^{(\ell)*} \left(D_n^{(\ell)} \right)$ generally admits no closed-form expression and is difficult to evaluate. To enable tractable expert selection, we introduce a deterministic surrogate by replacing the random fading term with its expectation. Specifically, we define $\tilde{E}_n^{(\ell)}(D) \triangleq$

$\mathbb{E} \left[\frac{1}{h} \right] \frac{\left(2^{\frac{bD}{B_n T_{\text{UE},n}^{(\ell)}}} - 1 \right) N_0 B_n T_{\text{UE},n}^{(\ell)}}{d_n^{-\alpha} G_{\text{UE},n}}$. The surrogate $\tilde{E}_n^{(\ell)}(D)$ corresponds to minimizing the expected energy over a restricted class of non-adaptive bit-allocation policies that do not exploit instantaneous fading variations. Since $E_n^{(\ell)*}(D)$ minimizes over all causal policies, the surrogate provides an upper bound: $E_n^{(\ell)*}(D) \leq \tilde{E}_n^{(\ell)}(D), \forall D$. Using this surrogate, the outer problem reduces to $\min_{\mathbf{X}} E_{\text{UE}}^{(\ell)} + \sum_{n \in \mathcal{N}} \tilde{E}_n^{(\ell)} \left(D_n^{(\ell)} \right)$, which has the same structural form as the slow-fading case and can therefore be solved using the proposed algorithms in Section IV.

C. Adaptive Transmission Strategy

After obtaining the optimal helper loads $\left\{ D_n^{(\ell)*} \right\}$ from the outer problem, the optimal slot-level bit allocation $\left\{ \gamma_{n,t}^{(\ell)} \right\}$ is recovered by solving the inner problem for helper n , which is given by

$$\mathcal{P}3_n: \quad \min_{\gamma^{(\ell)}} \mathbb{E}_h \left[\sum_{t=1}^{Q_n^{(\ell)}} E_{n,t}^{(\ell)} \left(\gamma_{n,t}^{(\ell)}, h_{n,t}^{(\ell)} \right) \right] \quad (24)$$

with the constraint $\sum_{t=1}^{Q_n^{(\ell)}} \gamma_{n,t}^{(\ell)} = b D_n^{(\ell)*}$.

Let $\beta_{n,t}^{(\ell)}$ denote the remaining number of bits to be transmitted to helper n at the beginning of time slot t during MoE layer ℓ . Using the approach of DP, the objective function of $\mathcal{P}3_n$ can be rewritten as

$$\begin{aligned} \mathcal{P}4_n: \quad & U_t \left(\beta_{n,t}^{(\ell)}, h_{n,t}^{(\ell)} \right) \\ & = \begin{cases} \min_{\gamma_{n,t}^{(\ell)} \leq \beta_{n,t}^{(\ell)}} E_{n,t}^{(\ell)} + \bar{U}_t \left(\beta_{n,t}^{(\ell)} - \gamma_{n,t}^{(\ell)} \right), & \text{if } 1 \leq t < Q_n^{(\ell)}, \\ \frac{\left(2^{a_n \beta_{n,t}^{(\ell)}} - 1 \right) c_n}{h_{n,t}^{(\ell)}}, & \text{if } t = Q_n^{(\ell)}, \end{cases} \end{aligned} \quad (25)$$

where $a_n = \frac{1}{B_n \tau}$, $c_n = \frac{N_0 B_n \tau}{d_n^{-\alpha} G_{\text{UE},n}}$. The cost-to-go function $\bar{U}_t \left(\beta_{n,t}^{(\ell)} \right) = \mathbb{E}_h \left[U_t \left(\beta_{n,t}^{(\ell)}, h_{n,t}^{(\ell)} \right) \right]$ denotes the expected energy consumption for transmitting $\beta_{n,t}^{(\ell)}$ bits over the remaining slots.

Theorem 3 (Optimal slot-level bit allocation under fast fading). Under fast-fading channels, considering a fixed helper n and a given load $D_n^{(\ell)}$ at MoE layer ℓ , the optimal bit allocation in slot t is given by

$$\begin{aligned} \gamma_{n,t}^{(\ell)*} & = \frac{1}{\left(Q_n^{(\ell)} - t + 1 \right) a_n} \\ & \cdot \left[a_n \beta_{n,t}^{(\ell)} + \sum_{j=0}^{Q_n^{(\ell)} - t - 1} \log_2 \left(h_{n,t}^{(\ell)} \mathbb{E} \left[\frac{1}{h_{n,Q-j}^{(\ell)}} \right] \right) \right]. \end{aligned} \quad (26)$$

The resulting minimum expected uplink energy consumption is given by

$$\begin{aligned} \tilde{E}_n^* \left(D_n^{(\ell)} \right) = c_n & \left[Q_n^{(\ell)} 2^{\frac{a_n D_n^{(\ell)}}{Q_n^{(\ell)}}} \left(\frac{1}{h_{n,1}^{(\ell)}} \prod_{t=2}^{Q_n^{(\ell)}} \mathbb{E} \left[\frac{1}{h_{n,t}^{(\ell)}} \right] \right) \right. \\ & \left. - \left(\frac{1}{h_{n,1}^{(\ell)}} + \sum_{t=2}^{Q_n^{(\ell)}} \mathbb{E} \left[\frac{1}{h_{n,t}^{(\ell)}} \right] \right) \right]. \end{aligned} \quad (27)$$

Proof. Please see Appendix D. \square

VI. EXPERIMENTAL RESULTS

A. Experimental Setup

In our simulations, we consider two types of MoE models, each with 8 experts per MoE layer. One is switch-base-8 [40], a switch transformer–based MoE model, which is tested on the Extreme Summarization (XSum) dataset [41]. Under the conventional score-based Top- K routing mechanism, each token is routed to a single expert at each layer (i.e., $K = 1$). The other is Mixtral-8×7B [9], a sparse MoE model with a 7B-parameter backbone, which is tested on the CommonsenseQA dataset [42]. Under the Top- K routing mechanism, each token is routed to two experts at each layer (i.e., $K = 2$). Expert loading and computing are conducted on an NVIDIA GeForce RTX 4090 GPU. The maximal distance between the edge device and its helpers is set as 150 m. The wireless parameters are set as follows [15]: The transmit power of helpers is 38 dBm. The path-loss factor is $\alpha = 4$, the antenna-related factor is 1, and the noise power spectral density is -174 dBm/Hz. The small-scale channel fading h is modeled as a Gamma-distributed fading variable with unit mean, where the shape parameter is set to 2 [43]. The hyperparameters introduced in Assumptions 1 and 2 can be empirically estimated using finite-difference tests following the lightweight approach in [44], [45].

To demonstrate the effectiveness of our proposed SiftMoE during WIDE inference, we compare SiftMoE with two benchmark schemes:

- **Ideal Top- K :** This benchmark follows the conventional score-based Top- K expert routing, where the outputs of all selected experts are always successfully received by the user within the given latency constraint. It therefore serves as an upper bound on the achievable inference accuracy.
- **(Practical) Top- K :** This scheme also adopts the conventional score-based Top- K routing but accounts for realistic wireless channel conditions. In this case, some expert outputs may fail to be delivered to the user within the latency budget, leading to degraded inference performance.

B. Effectiveness of SiftMoE and Accuracy-Energy Tradeoff

To validate the effectiveness of expert replacement or skipping in the proposed SiftMoE, we compare the inference accuracy and energy consumption of SiftMoE with those of the benchmark schemes under slow-fading channels, where

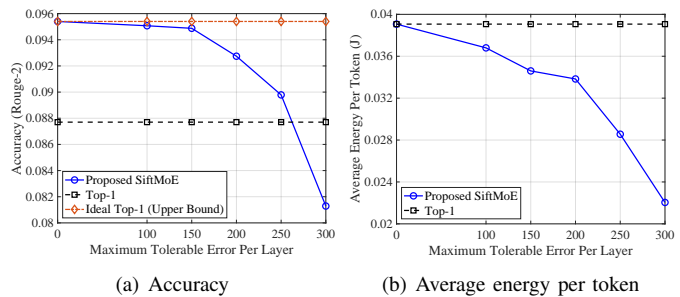


Fig. 3. Comparison under slow-fading channels for different maximum tolerable errors per layer on switch-base-8 over XSum, where $B_n = 1$ MHz and $T = 0.7$ s.

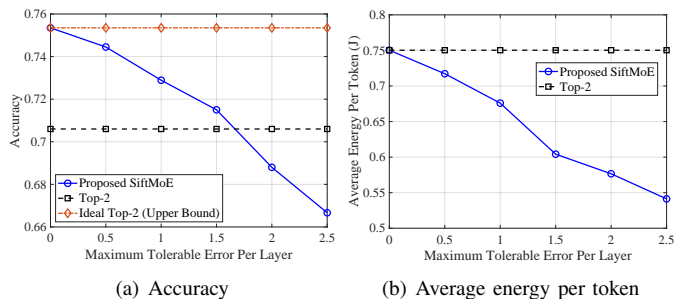


Fig. 4. Comparison under slow-fading channels for different maximum tolerable errors per layer on Mixtral-8×7B over CommonsenseQA, where $B_n = 2$ MHz and $T = 0.074$ s.

the impact of expert selection can be clearly observed. Fig. 3 illustrates the performance comparison on the switch-base-8 model over XSum under different maximum tolerable errors per layer. As shown in Fig. 3(a), when the maximum tolerable error is small, the accuracy achieved by SiftMoE is very close to that of the ideal Top-1 benchmark, indicating that the proposed SiftMoE introduces only limited accuracy degradation. When the maximum tolerable error increases, the accuracy of SiftMoE gradually decreases due to accumulated layer-wise deviations. However, within a moderate range of tolerant errors, SiftMoE consistently outperforms the practical Top-1 scheme that accounts for realistic channel conditions. Meanwhile, Fig. 3(b) shows that as the maximum tolerable error increases, the average energy consumption per token under SiftMoE decreases monotonically and remains significantly lower than that of Top-1 benchmark. Fig. 4 presents the corresponding results for the Mixtral-8×7B model on the CommonsenseQA dataset, where similar performance trends can be observed. These results demonstrate that by appropriately tuning the maximum tolerable error, SiftMoE enables a flexible accuracy–energy trade-off, where substantial energy savings can be achieved at the cost of controlled and predictable accuracy degradation.

C. Effects of System Parameters Under Slow Fading

To ensure a fair comparison, the maximum tolerable per-layer error is set to 200 for switch-base-8 and 1.5 for Mixtral-8×7B in the following simulations. Fig. 5 illustrates the effect of system constraints on the average energy consumption per token for switch-base-8 model over XSum under slow

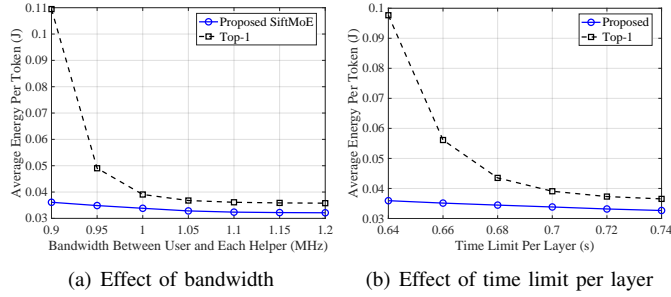


Fig. 5. Effect of system constraints on average energy consumption for switch-base-8 over XSum under slow fading. The default values of B_n and T are set to 1 MHz and 0.7 s.

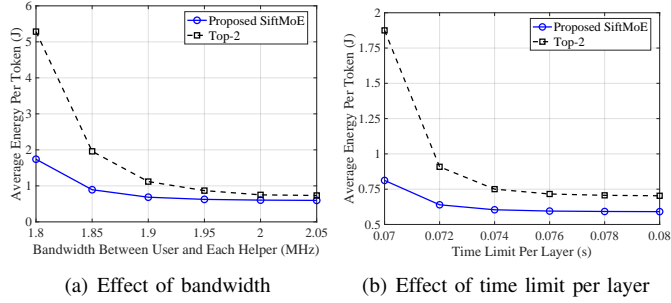


Fig. 6. Effect of system constraints on average energy consumption for Mixtral-8x7B over CommonsenseQA under slow fading. The default values of B_n and T are set to 2 MHz and 0.074 s.

fading. As shown in Fig. 5(a), when the user-helper bandwidth increases, the average energy consumption per token decreases for both schemes, owing to lower uplink transmission energy. Notably, SiftMoE consistently consumes significantly less energy than the Top-1 benchmark across the entire bandwidth range. This gap is particularly pronounced under limited bandwidth, where the fixed token-helper assignment in the conventional Top-1 scheme forces certain helpers to process a large number of tokens, leading to disproportionately high energy consumption. Fig. 5(b) shows the effect of the per-layer time limit. As the time limit increases, the energy consumption of both schemes decreases, since a looser latency constraint allows the user to transmit hidden states over a longer duration with lower transmission power. Fig. 6 presents similar trends for the Mixtral-8x7B model on the CommonsenseQA dataset. Nevertheless, SiftMoE consistently achieves lower energy consumption than Top- K under all considered bandwidth and latency constraints.

D. Effects of System Parameters Under Fast Fading

We next evaluate the energy performance of SiftMoE under fast fading channels. Fig. 7 shows the effect of system constraints on the average energy consumption for the switch-base-8 model over XSum under fast fading. Here, Prop. Dynamic denotes the proposed adaptive transmission strategy that dynamically adjusts the amount of transmitted data in each time slot according to the instantaneous small-scale fading, while Uniform corresponds to a baseline scheme that allocates an equal amount of data transmission across all time slots.

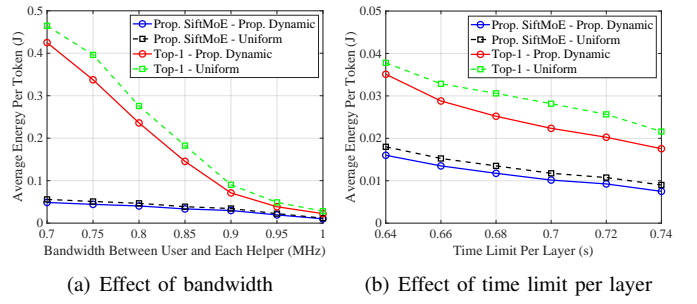


Fig. 7. Effect of system constraints on average energy consumption for switch-base-8 over XSum under fast fading. The default values of B_n and T are set to 1 MHz and 0.7 s.

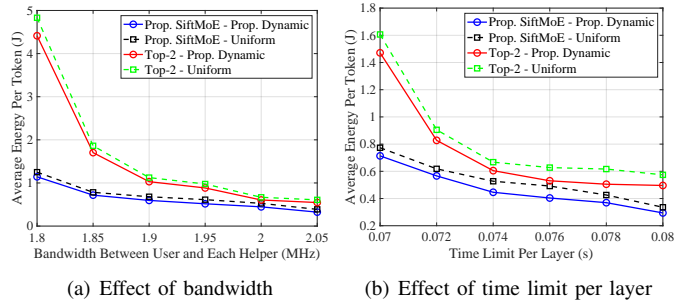


Fig. 8. Effect of system constraints on average energy consumption for Mixtral-8x7B over CommonsenseQA under fast fading. The default values of B_n and T are set to 2 MHz and 0.074 s.

As shown in Fig. 7(a), increasing the user-helper bandwidth reduces the energy consumption for all schemes. Compared with the uniform transmission strategy, the proposed dynamic scheme consistently achieves lower energy consumption by exploiting favorable channel realizations to transmit data with lower energy. Moreover, SiftMoE with dynamic transmission significantly outperforms the Top-1 baselines across the entire bandwidth range, with more pronounced gains under tight bandwidth constraints. Similar trends can be observed in Fig. 7(b) with respect to the per-layer time limit, where relaxing the latency constraint further reduces energy consumption, and the proposed dynamic strategy consistently outperforms uniform transmission under fast fading. Fig. 8 shows the corresponding results for the Mixtral-8x7B model on the CommonsenseQA dataset, exhibiting consistent performance trends across both bandwidth and time-limit variations. Overall, these results confirm that under fast fading, combining expert selection flexibility with channel-aware dynamic transmission is key to achieving energy-efficient MoE inference.

VII. CONCLUSION REMARKS

In this paper, we revisited distributed MoE inference over wireless edge networks from an energy-efficiency perspective. Rather than strictly adhering to the conventional Top- K routing paradigm, we showed that allowing similarity-aware expert replacement and skipping opens a new research direction for communication-efficient WIDE inference. Our analysis reveals that the impact of expert selection on inference accuracy can be theoretically characterized by layer-wise deviation bounds,

thereby enabling control of the accuracy–energy tradeoff. Building on this insight, we developed the SiftMoE framework that integrates expert selection with wireless resource considerations. The results demonstrate that substantial energy savings can be achieved while maintaining controllable accuracy degradation, highlighting the potential of communication-aware expert selection as a practical mechanism for deploying MoE models in wireless edge networks.

Several directions deserve further investigation. First, we can extend the current framework to multi-user scenarios, which would introduce additional competition not only among tokens within a user but also across different users sharing communication and computing resources. Second, while this work focuses on expert replacement and skipping within each MoE layer, exploring whether entire MoE layers can be selectively skipped may further reduce communication overhead. Finally, integrating hidden-state transmission with advanced physical-layer techniques such as over-the-air computation may further improve the efficiency of WIDE inference.

APPENDIX A PROOF OF PROPOSITION 1

By definition, the deviation induced by expert substitution at layer ℓ is given by $\tilde{y}^{(\ell)}(z) - y_{\text{Top}}^{(\ell)}(z) = \sum_{i \in \mathcal{A}_{\text{Top}}^{(\ell)}(z)} g_i^{(\ell)}(z) \left(\text{FFN}_{\varphi(i)}^{(\ell)}(z) - \text{FFN}_i^{(\ell)}(z) \right)$.

To further characterize the effect of this deviation, we measure the deviation magnitude using the l_2 -norm. Then, $\delta^{(\ell)}(z)$ can be upper-bounded as

$$\begin{aligned} \delta^{(\ell)}(z) &\leq \sum_{i \in \mathcal{A}_{\text{Top}}^{(\ell)}(z)} \left\| g_i^{(\ell)}(z) \left(\text{FFN}_{\varphi(i)}^{(\ell)}(z) - \text{FFN}_i^{(\ell)}(z) \right) \right\|_2 \\ &= \sum_{i \in \mathcal{A}_{\text{Top}}^{(\ell)}(z)} g_i^{(\ell)}(z) \left\| \text{FFN}_{\varphi(i)}^{(\ell)}(z) - \text{FFN}_i^{(\ell)}(z) \right\|_2 \\ &= \sum_{i \in \mathcal{A}_{\text{Top}}^{(\ell)}(z)} g_i^{(\ell)}(z) \left\| \text{FFN}_i^{(\ell)}(z) \right\|_2 \\ &\quad \cdot \sqrt{1 + \rho_{i,\varphi(i)}^{(\ell)}(z)^2 - 2\rho_{i,\varphi(i)}^{(\ell)}(z) \cos \theta_{i,\varphi(i)}^{(\ell)}(z)}. \end{aligned} \quad (28)$$

Then, the expected deviation magnitude at layer ℓ satisfies $\mathbb{E} \left[\delta^{(\ell)}(z) \right] \leq \sum_{i \in \mathcal{A}_{\text{Top}}^{(\ell)}(z)} g_i^{(\ell)}(z) \mathbb{E} \left[F_{i,\varphi(i)}^{(\ell)}(z) \right]$.

APPENDIX B PROOF OF THEOREM 1

At layer ℓ , the discrepancy between the substituted output and the original output can be decomposed into (A) an

amplification of the input deviation and (B) the intrinsic error introduced by expert selection at the current layer.

$$\begin{aligned} e^{(\ell)} &= \left\| \tilde{y}^{(\ell)} \left(\tilde{y}^{(\ell-1)} \right) - y_{\text{Top}}^{(\ell)} \left(y_{\text{Top}}^{(\ell-1)} \right) \right\|_2 \\ &= \left\| \underbrace{\tilde{y}^{(\ell)} \left(\tilde{y}^{(\ell-1)} \right) - \tilde{y}^{(\ell)} \left(y_{\text{Top}}^{(\ell-1)} \right)}_{\text{(A)}} \right. \\ &\quad \left. + \underbrace{\tilde{y}^{(\ell)} \left(y_{\text{Top}}^{(\ell-1)} \right) - y_{\text{Top}}^{(\ell)} \left(y_{\text{Top}}^{(\ell-1)} \right)}_{\text{(B)}} \right\|_2 \\ &\leq \left\| \tilde{y}^{(\ell)}(\tilde{z}) - \tilde{y}^{(\ell)}(z) \right\|_2 + \delta^{(\ell)}, \end{aligned} \quad (29)$$

where we have set $z \triangleq y_{\text{Top}}^{(\ell-1)}$ and $\tilde{z} \triangleq \tilde{y}^{(\ell-1)}$.

We first analyze the propagated input deviation term. Using the MoE structure of the substituted layer, the difference $\tilde{y}^{(\ell)}(\tilde{z}) - \tilde{y}^{(\ell)}(z)$ can be expanded as the sum of two components: $\tilde{y}^{(\ell)}(\tilde{z}) - \tilde{y}^{(\ell)}(z) = \sum_{i \in \mathcal{E}^{(\ell)}} g_i^{(\ell)}(\tilde{z}) \text{FFN}_i^{(\ell)}(\tilde{z}) - \sum_{i \in \mathcal{E}^{(\ell)}} g_i^{(\ell)}(z) \text{FFN}_i^{(\ell)}(z) = \sum_{i \in \mathcal{E}^{(\ell)}} \left(g_i^{(\ell)}(\tilde{z}) - g_i^{(\ell)}(z) \right) \text{FFN}_i^{(\ell)}(\tilde{z}) + \sum_{i \in \mathcal{E}^{(\ell)}} g_i^{(\ell)}(z) \left(\text{FFN}_i^{(\ell)}(\tilde{z}) - \text{FFN}_i^{(\ell)}(z) \right)$. Using the norm property for scalar and applying the triangle inequality, we obtain that

$$\begin{aligned} &\left\| \tilde{y}^{(\ell)}(\tilde{z}) - \tilde{y}^{(\ell)}(z) \right\|_2 \\ &\leq \underbrace{\sum_{i \in \mathcal{E}^{(\ell)}} \left| g_i^{(\ell)}(\tilde{z}) - g_i^{(\ell)}(z) \right| \left\| \text{FFN}_i^{(\ell)}(\tilde{z}) \right\|_2}_{T_a^{(\ell)}} \\ &\quad + \underbrace{\sum_{i \in \mathcal{E}^{(\ell)}} g_i^{(\ell)}(z) \left\| \text{FFN}_i^{(\ell)}(\tilde{z}) - \text{FFN}_i^{(\ell)}(z) \right\|_2}_{T_b^{(\ell)}}. \end{aligned} \quad (30)$$

We first focus on the term $T_a^{(\ell)}$ in (30), which captures the error induced by the variation of the gating scores under input deviation. Applying the triangle inequality and using Assumption 1, we factor out the maximum expert output norm and obtain, we obtain the following upper bound, given by

$$\begin{aligned} T_a^{(\ell)} &\leq \left(\sum_{i \in \mathcal{E}^{(\ell)}} \left| g_i^{(\ell)}(\tilde{z}) - g_i^{(\ell)}(z) \right| \right) \cdot \max_{i \in \mathcal{E}^{(\ell)}} \left\| \text{FFN}_i^{(\ell)}(\tilde{z}) \right\|_2 \\ &= \left\| \Delta g^{(\ell)} \right\|_1 \cdot B_{\max}^{(\ell)}, \end{aligned} \quad (31)$$

where $\Delta g^{(\ell)}$ denotes the vector of gating-weight differences with entries $\Delta g_i^{(\ell)} = g_i^{(\ell)}(\tilde{z}) - g_i^{(\ell)}(z)$. In addition, $\left\| \Delta g^{(\ell)} \right\|_1$ has the following upper bound: $\left\| \Delta g^{(\ell)} \right\|_1 \leq \sum_{i \in \mathcal{E}^{(\ell)}} \left(g_i^{(\ell)}(\tilde{z}) + g_i^{(\ell)}(z) \right) = \sum_{i \in \mathcal{E}^{(\ell)}} g_i^{(\ell)}(\tilde{z}) + \sum_{i \in \mathcal{E}^{(\ell)}} g_i^{(\ell)}(z) = 2$. Therefore, $T_a \leq 2B_{\max}^{(\ell)}$ holds.

Next, we bound the term $T_b^{(\ell)}$ in (30), which captures the output deviation caused by passing a perturbed hidden

representation through the same set of experts. Since the gating scores satisfy $\sum_{i \in \mathcal{E}(\ell)} g_i^{(\ell)}(z) = 1$, with Assumption 2, $T_b^{(\ell)}$ has the following upper bound:

$$T_b^{(\ell)} \leq \sum_{i \in \mathcal{E}(\ell)} g_i^{(\ell)}(z) \beta_{E,i}^{(\ell)} \|\tilde{z} - z\|_2 \leq \beta_{E,\max}^{(\ell)} \|\tilde{z} - z\|_2. \quad (32)$$

By first substituting (31) and (32) into (30), and then substituting the result into (29), we obtain $e^{(\ell)} \leq \beta_{E,\max}^{(\ell)} e^{(\ell-1)} + 2B_{\max}^{(\ell)} + \delta^{(\ell)}$. By setting $e^{(0)} = 0$ and unrolling this recursion over the first ℓ layers, we obtain the following bound on the output deviation at layer ℓ : $e^{(L)} \leq \sum_{r=1}^{\ell} (2B_{\max}^{(r)} + \delta^{(r)}) \prod_{t=r+1}^{\ell} \beta_{E,\max}^{(t)}$.

APPENDIX C PROOF OF PROPOSITION 2

From (3), it is straightforward to observe that $E_{\text{UE}}^{(\ell)}$ increases linearly with $D_{\text{UE}}^{(\ell)}$. Hence, we focus on characterizing the relationship between the helper-side energy consumption $E_n^{(\ell)}$ and $D_n^{(\ell)}$.

Although $D_n^{(\ell)}$ is an integer-valued decision variable in the considered subproblem, we first relax it to a continuous variable $D_n^{(\ell)} \in \mathbb{R}_+$ and study the convexity of $E_n^{(\ell)}(D_n^{(\ell)})$ over the continuous domain. This relaxation is introduced solely for analytical purposes.

For notation simplicity, we define $\gamma_n^{(\ell)} = \frac{\phi}{C_n} + \frac{b}{R_{n,\text{UE}}^{(\ell)}}$. Let $u_n^{(\ell)} = T - \gamma_n^{(\ell)} D_n^{(\ell)}$, then the objective function can be rewritten as a composite function $E_n^{(\ell)}(D_n^{(\ell)}) = \psi(u_n^{(\ell)})$, where $\psi(u_n^{(\ell)}) = \left[2^{\frac{b}{B_n \gamma_n^{(\ell)}} \left(\frac{T}{u_n^{(\ell)}} - 1 \right)} - 1 \right] u_n^{(\ell)} = 2^{-\frac{b}{B_n \gamma_n^{(\ell)}}} e^{\frac{bT \ln 2}{B_n \gamma_n^{(\ell)} u_n^{(\ell)}}} u_n^{(\ell)} - u_n^{(\ell)}$.

We first analyze the properties of $\psi(u_n^{(\ell)})$. The first-order derivative of $\psi(u_n^{(\ell)})$ is given by $\psi'(u_n^{(\ell)}) = 2^{-\frac{b}{B_n \gamma_n^{(\ell)}}} e^{\frac{bT \ln 2}{B_n \gamma_n^{(\ell)} u_n^{(\ell)}}} \left(1 - \frac{bT \ln 2}{B_n \gamma_n^{(\ell)} u_n^{(\ell)}} \right) - 1$. To characterize its sign, we define an auxiliary function $f(x) = e^x(1-x)$. Its derivative satisfies $f'(x) = -xe^x < 0$ for all $x > 0$, implying that $f(x)$ is strictly decreasing when $x > 0$ and hence $f(x) < f(0) = 1$. Consequently, $e^{\frac{bT \ln 2}{B_n \gamma_n^{(\ell)} u_n^{(\ell)}}} \left(1 - \frac{bT \ln 2}{B_n \gamma_n^{(\ell)} u_n^{(\ell)}} \right) < 1$. Since $2^{-\frac{b}{B_n \gamma_n^{(\ell)}}} < 1$, it follows that $\psi'(u_n^{(\ell)}) < 0$ for all $u_n^{(\ell)} > 0$.

Moreover, the second-order derivative of $\psi(u_n^{(\ell)})$ is $\psi''(u_n^{(\ell)}) = 2^{-\frac{b}{B_n \gamma_n^{(\ell)}}} e^{\frac{bT \ln 2}{B_n \gamma_n^{(\ell)} u_n^{(\ell)}}} \left(\frac{bT \ln 2}{B_n \gamma_n^{(\ell)}} \right)^2 \frac{1}{(u_n^{(\ell)})^3}$, which is strictly positive for all $u_n^{(\ell)} > 0$. Therefore, $\psi(u_n^{(\ell)})$ is a decreasing and convex function with respect to $u_n^{(\ell)}$.

Next, we examine the monotonicity and convexity of the composite function $\psi(u(D_n^{(\ell)}))$, i.e., $E(D_n^{(\ell)})$. Note that $u'(D_n^{(\ell)}) = -\gamma_n^{(\ell)} < 0$ and $u''(D_n^{(\ell)}) = 0$. By the chain rule, the first-order derivative of $E_n^{(\ell)}(D_n^{(\ell)})$ is $\frac{dE_n^{(\ell)}(D_n^{(\ell)})}{dD_n^{(\ell)}} = \psi'(u(D_n^{(\ell)})) \cdot u'(D_n^{(\ell)}) > 0$. Furthermore, the second-order derivative satisfies $\frac{d^2 E_n^{(\ell)}(D_n^{(\ell)})}{d(D_n^{(\ell)})^2} = \psi''(u(D_n^{(\ell)}))$.

$(u'(D_n^{(\ell)}))^2 + \psi'(u(D_n^{(\ell)})) \cdot u''(D_n^{(\ell)}) > 0$. Hence, $E(D_n^{(\ell)})$ is an increasing and convex function of $D_n^{(\ell)}$ over the continuous domain $D_n^{(\ell)} \in \mathbb{R}_+$.

Finally, when $D_n^{(\ell)}$ is restricted to integer values with unit spacing, the discrete sequence $\{E_n^{(\ell)}(D_n^{(\ell)})\}_{D_n^{(\ell)} \in \mathbb{Z}_+}$ preserves these properties. Specifically, the monotonicity of $E_n^{(\ell)}(D_n^{(\ell)})$ implies $E_n^{(\ell)}(D_n^{(\ell)} + 1) - E_n^{(\ell)}(D_n^{(\ell)}) > 0$, and the convexity of $E_n^{(\ell)}(D_n^{(\ell)})$ over the continuous domain further guarantees that the second-order finite difference is nonnegative, i.e., $E_n^{(\ell)}(D_n^{(\ell)} + 1) - E_n^{(\ell)}(D_n^{(\ell)}) > E_n^{(\ell)}(D_n^{(\ell)}) - E_n^{(\ell)}(D_n^{(\ell)} - 1)$ for any $D_n^{(\ell)} \geq 1$. Therefore, $E_n^{(\ell)}$ is a non-decreasing discrete convex function with respect to $D_n^{(\ell)}$.

APPENDIX D PROOF OF THEOREM 3

We take the transmission strategy to a specific helper n and an MoE layer ℓ as an example. Thus, we omit the index of helper n and layer ℓ and only leave the index of time slot t . Then, we have $\bar{U}_Q(\beta_Q) = \mathbb{E}_h[U_Q(\beta_Q, h_Q)] = c(2^{a\beta_Q} - 1) \mathbb{E}\left[\frac{1}{h_Q}\right]$.

The optimal transmitted bits in slot $(Q-1)$, i.e., γ_{Q-1}^* , is given by $\gamma_{Q-1}^* = \arg \min_{\gamma_{Q-1}} \frac{c(2^{a\beta_{Q-1}} - 1)}{h_{Q-1}} + c[2^{a(\beta_{Q-1} - \gamma_{Q-1})} - 1] \mathbb{E}\left[\frac{1}{h_Q}\right] = \frac{1}{2a} \left[a\beta_{Q-1} + \log_2 \left(h_{Q-1} \mathbb{E}\left[\frac{1}{h_Q}\right] \right) \right]$, and the cost-to-go function is $U_{Q-1}(\beta_{Q-1}, h_{Q-1}) = c \left[2 \cdot 2^{\frac{a\beta_{Q-1}}{2}} \left(\frac{1}{h_{Q-1}} \mathbb{E}\left[\frac{1}{h_Q}\right] \right)^{\frac{1}{2}} - \left(\frac{1}{h_{Q-1}} + \mathbb{E}\left[\frac{1}{h_Q}\right] \right) \right]$.

Calculating the above repeatedly, we can obtain the optimal transmitted bits as $\gamma_{Q-i}^* = \frac{1}{(i+1)a} \left[a\beta_{Q-i} + \sum_{j=0}^{i-1} \log_2 \left(h_{Q-i} \mathbb{E}\left[\frac{1}{h_{Q-j}}\right] \right) \right]$. Then, $U_{Q-i}^* = c \left[(i+1) 2^{\frac{a\beta_{Q-i}}{i+1}} \left(\frac{1}{h_{Q-i}} \prod_{j=0}^{i-1} \mathbb{E}\left[\frac{1}{h_{Q-j}}\right] \right)^{\frac{1}{i+1}} - \left(\frac{1}{h_{Q-i}} + \sum_{j=0}^{i-1} \mathbb{E}\left[\frac{1}{h_{Q-j}}\right] \right) \right]$ holds. Let $Q-i = 1$ and $\beta_{Q-i} = D$, the proof is completed.

REFERENCES

- [1] W. X. Zhao, K. Zhou, J. Li, T. Tang, X. Wang, Y. Hou, Y. Min, B. Zhang, J. Zhang, Z. Dong *et al.*, "A survey of large language models," *arXiv preprint arXiv:2303.18223*, vol. 1, no. 2, 2023.
- [2] C. Wu, X. Wang, Y. Hu, S. Han, W. Meng, and D. Niyato, "Towards intelligent SAGIN: Leveraging big AI models and SDN for end-to-end automation," *to appear in IEEE Netw.*, 2025.
- [3] G. Qu, Q. Chen, W. Wei, Z. Lin, X. Chen, and K. Huang, "Mobile edge intelligence for large language models: A contemporary survey," *IEEE Commun. Surveys Tuts.*, vol. 27, no. 6, pp. 3820–3860, Dec. 2025.
- [4] Z. Lin, G. Qu, Q. Chen, X. Chen, Z. Chen, and K. Huang, "Pushing large language models to the 6G edge: Vision, challenges, and opportunities," *IEEE Commun. Mag.*, vol. 63, no. 9, pp. 52–59, Sep. 2025.
- [5] F. Wang, S. Zhang, E.-K. Hong, and T. Q. S. Quek, "Constellation as a service: Tailored connectivity management in direct-satellite-to-device networks," *IEEE Commun. Mag.*, vol. 63, no. 11, pp. 30–36, Nov. 2025.
- [6] Y. Zheng, Y. Chen, B. Qian, X. Shi, Y. Shu, and J. Chen, "A review on edge large language models: Design, execution, and applications," *ACM Comput. Surv.*, vol. 57, no. 8, pp. 1–35, Aug. 2025.
- [7] G. Qu, Z. Lin, Q. Chen, J. Li, F. Liu, X. Chen, and K. Huang, "Trim-Caching: Parameter-sharing edge caching for AI model downloading," *arXiv preprint arXiv:2404.14204*, 2024.
- [8] Q. Chen, Z. Wang, X. Chen, J. Wen, D. Zhou, S. Ji, M. Sheng, and K. Huang, "Space-ground fluid AI for 6G edge intelligence," *Engineering*, vol. 54, no. 11, pp. 14–19, Nov. 2025.

- [9] A. Q. Jiang, A. Sablayrolles, A. Roux, A. Mensch, B. Savary, C. Bamford, D. S. Chaplot, D. d. l. Casas, E. B. Hanna, F. Bressand *et al.*, “Mixture of experts,” *arXiv preprint arXiv:2401.04088*, 2024.
- [10] C. Gao, K. Chen, J. Rao, R. Liu, B. Sun, Y. Zhang, D. Peng, X. Guo, and V. Subrahmanian, “MoLA: MoE LoRA with layer-wise expert allocation,” in *Proc. Findings of the Association for Computational Linguistics: NAACL 2025*, Albuquerque, New Mexico, Apr.-May 2025, pp. 5097–5112.
- [11] R. Kong, Y. Li, W. Wang, L. Kong, and Y. Liu, “Serving MoE models on resource-constrained edge devices via dynamic expert swapping,” *IEEE Trans. Comput.*, vol. 74, no. 8, pp. 2799–2811, Aug. 2025.
- [12] R. Yi, L. Guo, S. Wei, A. Zhou, S. Wang, and M. Xu, “EdgeMoE: Empowering sparse large language models on mobile devices,” *IEEE Trans. Mobile Comput.*, vol. 24, no. 8, pp. 7059–7073, Aug. 2025.
- [13] G. Qu, T. Li, Q. Chen, X. Chen, and S. Zhou, “SLIDE: Simultaneous model downloading and inference at the wireless network edge,” *arXiv preprint arXiv:2512.20946*, 2025.
- [14] Z. Zhang, Y. Xia, H. Wang, D. Yang, C. Hu, X. Zhou, and D. Cheng, “MPMoE: Memory efficient MoE for pre-trained models with adaptive pipeline parallelism,” *IEEE Trans. Parallel Distrib. Syst.*, vol. 35, no. 6, pp. 998–1011, Jun. 2024.
- [15] Q. Chen, X. Chen, and K. Huang, “SlimCaching: Edge caching of mixture-of-experts for distributed inference,” to appear in *IEEE Trans. Mobile Comput.*, 2026.
- [16] Z. Liu, X. Wang, C. Feng, X. Sun, W. Zhan, and X. Chen, “Meta-reinforcement learning with mixture of experts for generalizable multi access in heterogeneous wireless networks,” *IEEE Trans. Commun.*, vol. 74, pp. 870–885, 2026.
- [17] Q. Song, S. Jing, S. Zhang, S. Zhang, and C. Huang, “Mixture-of-experts for distributed edge computing with channel-aware gating function,” in *Proc. IEEE Int. Conf. Commun. Workshops (ICC Workshops)*, Montreal, Canada, Jun. 2025, pp. 1353–1358.
- [18] Z. Fang, Z. Lin, S. Hu, Y. Ma, Y. Tao, Y. Deng, X. Chen, and Y. Fang, “HFedMoE: Resource-aware heterogeneous federated learning with mixture-of-experts,” *arXiv preprint arXiv:2601.00583*, 2026.
- [19] V. Gupta, K. Sinha, A. Gavrilovska, and A. P. Iyer, “LYNX: Enabling efficient MoE inference through dynamic batch-aware expert selection,” *arXiv preprint arXiv:2411.08982*, 2024.
- [20] X. Lu, Q. Liu, Y. Xu, A. Zhou, S. Huang, B. Zhang, J. Yan, and H. Li, “Not all experts are equal: Efficient expert pruning and skipping for mixture-of-experts large language models,” in *Proc. Annual Meeting of the Association for Computational Linguistics (ACL)*, Bangkok, Thailand, Aug. 2024, pp. 6159–6172.
- [21] P. Li, Z. Zhang, P. Yadav, Y.-L. Sung, Y. Cheng, M. Bansal, and T. Chen, “Merge, then compress: Demystify efficient SMOE with hints from its routing policy,” in *Proc. Int. Conf. Learn. Represent. (ICLR)*, Vienna, Austria, May 2024.
- [22] L. Li, Z. Qiyuan, J. Wang, W. Li, H. Gu, S. Han, and Y. Guo, “Sub-MoE: Efficient mixture-of-expert llms compression via subspace expert merging,” *arXiv preprint arXiv:2506.23266*, 2025.
- [23] Q. Huang, Z. An, N. Zhuang, M. Tao, C. Zhang, Y. Jin, K. Xu, K. Xu, L. Chen, S. Huang, and Y. Feng, “Harder task needs more experts: Dynamic routing in MoE models,” in *Proc. Annu. Meet. Assoc. Comput. Linguist. (ACL)*, Bangkok, Thailand, Aug. 2024, pp. 12 883–12 895.
- [24] S. Zhong, L. Liang, Y. Wang, R. Wang, R. Huang, and M. Li, “AdapMoE: Adaptive sensitivity-based expert gating and management for efficient MoE inference,” in *Proc. IEEE/ACM Int. Conf. Comput.-Aided Des. (ICCAD)*, New York, USA, Oct. 2024.
- [25] G. Zhu, M. Li, H. Dai, X. Liu, W. Wang, K. Li, L. Chen, W. Wang *et al.*, “Enabling MoE on the edge via importance-driven expert scheduling,” *arXiv preprint arXiv:2508.18983*, 2025.
- [26] G. Qu, Q. Chen, X. Chen, K. Huang, and Y. Fang, “PartialLoading: User scheduling and bandwidth allocation for parameter-sharing edge inference,” *arXiv preprint arXiv:2503.22982*, 2025.
- [27] N. Xue, Y. Sun, Z. Chen, M. Tao, X. Xu, L. Qian, S. Cui, W. Zhang, and P. Zhang, “WDMoE: Wireless distributed mixture of experts for large language models,” *IEEE Trans. Wireless Commun.*, vol. 25, pp. 559–572, Jan. 2026.
- [28] S. Qin, H. Wu, H. Du, and K. Huang, “Optimal expert selection for distributed mixture-of-experts at the wireless edge,” *arXiv preprint arXiv:2503.13421*, 2025.
- [29] K. M. Lo, Z. Huang, Z. Qiu, Z. Wang, and J. Fu, “A closer look into mixture-of-experts in large language models,” in *Findings of the Association for Computational Linguistics*, Albuquerque, New Mexico, Apr. 2025, pp. 4427–4447.
- [30] Y. Huang, Z. Wang, Z. Yuan, Y. Ding, R. Gong, J. Guo, X. Liu, and J. Zhang, “MoDES: Accelerating mixture-of-experts multimodal large language models via dynamic expert skipping,” *arXiv preprint arXiv:2511.15690*, 2025.
- [31] H. Li and L. Duan, “Theoretical analysis of mixture-of-experts in mobile edge computing,” *IEEE/ACM Trans. Netw.*, vol. 34, pp. 1569–1581, 2026.
- [32] S. Luo, R. Zhang, and T. J. Lim, “Downlink and uplink energy minimization through user association and beamforming in C-RAN,” *IEEE Trans. Wireless Commun.*, vol. 14, no. 1, pp. 494–508, Jan. 2015.
- [33] M. Chen, Z. Yang, W. Saad, C. Yin, H. V. Poor, and S. Cui, “A joint learning and communications framework for federated learning over wireless networks,” *IEEE Trans. Wireless Commun.*, vol. 20, no. 1, pp. 269–283, Jan. 2021.
- [34] Q. Zeng, Y. Du, K. Huang, and K. K. Leung, “Energy-efficient resource management for federated edge learning with CPU-GPU heterogeneous computing,” *IEEE Trans. Wireless Commun.*, vol. 20, no. 12, pp. 7947–7962, Dec. 2021.
- [35] Z. Chen, G. Fang, and W. Yu, “On non-asymptotic theory of recurrent neural networks in temporal point processes,” *J. Mach. Learn. Res.*, vol. 26, no. 154, pp. 1–67, Jul. 2025.
- [36] K. Scaman and A. Virmaux, “Lipschitz regularity of deep neural networks: analysis and efficient estimation,” in *Proc. Neural Inf. Process. Syst. (NeurIPS)*, Montréal, Canada, Dec. 2018, p. 3839–3848.
- [37] M. Mohri and A. Rostamizadeh, “Stability bounds for non-iid processes,” *Proc. Neural Inf. Process. Syst. (NeurIPS)*, Dec. 2007.
- [38] R. K. Ahuja, T. L. Magnanti, and J. B. Orlin, *Network Flows: Theory, Algorithms, and Applications*. Prentice Hall, 1993.
- [39] R. Bellman, *Dynamic Programming*. Princeton University Press, 1957.
- [40] W. Fedus, B. Zoph, and N. Shazeer, “Switch transformers: Scaling to trillion parameter models with simple and efficient sparsity,” *Journal of Machine Learning Research*, vol. 23, no. 120, pp. 1–39, 2022.
- [41] S. Narayan, S. B. Cohen, and M. Lapata, “Don’t give me the details, just the summary! Topic-aware convolutional neural networks for extreme summarization,” in *Proc. Empirical Methods in Natural Language Processing*, Brussels, Belgium, Oct.-Nov. 2018, pp. 1797–1807.
- [42] A. Talmor, J. Herzig, N. Lourie, and J. Berant, “CommonsenseQA: A question answering challenge targeting commonsense knowledge,” in *Proc. North American Chapter of the Association for Computational Linguistics: Human Language Technologies*, Minneapolis, Minnesota, Jun. 2019, pp. 4149–4158.
- [43] S.-W. Ko, K. Huang, S.-L. Kim, and H. Chae, “Live prefetching for mobile computation offloading,” *IEEE Trans. Wireless Commun.*, vol. 16, no. 5, pp. 3057–3071, May 2017.
- [44] Q. Chen, X. Chen, and K. Huang, “FedMeld: A model-dispersal federated learning framework for space-ground integrated networks,” to appear in *IEEE Trans. Mobile Comput.*, 2025.
- [45] W. Wei, Z. Lin, X. Liu, H. Du, D. Niyato, and X. Chen, “Optimizing split federated learning with unstable client participation,” *arXiv preprint arXiv:2509.17398*, 2025.